J Nanopart Res (2016) 18:63
DOI 10.1007/s11051-016-3366-5

RESEARCH PAPER

Synthesis of hierarchical MoS_2 microspheres composed of nanosheets assembled via facile hydrothermal method as anode material for lithium-ion batteries

Yongguang Zhang · Yue Li · Haipeng Li · Fuxing Yin · Yan Zhao · Zhumabay Bakenov

Received: 15 September 2015 / Accepted: 10 February 2016 / Published online: 24 February 2016

Abstract A hierarchical MoS_2 architecture composed of nanosheet-assembled microspheres with an expanded interplanar spacing of the (002) planes was successfully prepared via a simple hydrothermal reaction. Electron microscopy studies revealed formation of the MoS_2 microspheres with an average diameter of 230 nm. It was shown that the hierarchical structure of MoS_2 microspheres possesses both the merits of nanometer-sized building blocks and micrometer-sized assemblies, which offer high surface area for fast kinetics and buffers the volume expansion during lithium insertion/deinsertion, respectively. The micrometer-sized assemblies were found to contribute to the enhanced electrochemical stabilities of the electrode materials. The mentioned advantages of the MoS_2 electrode prepared in this work allowed enhanced cyclability and high rate capability of the material. Along with this, the material delivered a high initial discharge capacity of 1206 mAh g^{-1} and a reversible discharge capacity of 653 mAh g^{-1} after 100 cycles at a current density of 100 mA g^{-1}. Furthermore, the material delivered a high reversible capacity of 480 mAh g^{-1} at a high current density of 1000 mA g^{-1}.

Keywords Lithium-ion battery · Nanocomposite materials · Energy storage · MoS_2 anode · Hierarchical MoS_2 microspheres · Hydrothermal synthesis

Y. Zhang · Y. Li · H. Li (✉) · F. Yin · Y. Zhao
Research Institute for Energy Equipment Materials, Hebei University of Technology, Tianjin 300130, China
e-mail: lihp_hebut@outlook.com

Y. Zhang · Y. Li · H. Li · F. Yin · Y. Zhao
Tianjin Key Laboratory of Laminating Fabrication and Interface Control Technology for Advanced Materials, Hebei University of Technology, Tianjin 300130, China

Y. Li · H. Li
School of Material Science & Engineering, Hebei University of Technology, Tianjin 300130, China

Z. Bakenov
Institute of Batteries LLC, PI Nazarbayev University Research and Innovation System, Nazarbayev University, 53 Kabanbay Batyr Avenue, Astana 010000, Kazakhstan

Introduction

Rapid development of portable electronics and a wide implementation of electricity-powered transport along with expansion of the renewable energy sources use and integration into the electric grids, demand for high-performance and reliable power storage and conversion systems. Lithium-ion batteries (LIBs) lead the path for such devices, and many efforts have been devoted to develop the next generation of anode materials for LIBs with both high specific capacity and high energy density. Theoretical capacity of a common commercial anode, graphite, is 372 mAh g^{-1}, which is relatively low especially considering the recent development of high capacity cathodes for

example sulfur (Zhao et al. 2012; Zhang et al. 2011; Birrozzi et al. 2014). Therefore, development of advanced anode materials attracts great attention of the researchers worldwide. Among them, metal sulfides are promising material due to their high capacities (Zhong et al. 2012; Vaughn et al. 2012; Lai et al. 2012; Liu et al. 2012a; Gu et al. 2013; Fei et al. 2013). Molybdenum disulfide (MoS_2) is an "inorganic analogue of graphene", which has drawn particular research interest: it has a very high capacity about 670 mAh g^{-1} upon insertion of 4 mol of Li^+ (Wang et al. 2013). This material can accommodate lithium cations at lower potential through conversion reaction, and thus it can be used as anode material paired with high voltage (>4 V) lithiated cathodes (Sen and Mitra 2013). Despite these advantages, poor electrical/ionic conductivity of MoS_2 prevents achieving its full capacity, and the large volume changes upon reversible lithiation/delithiation leads to the material degradation and rapid capacity fading. Therefore tremendous efforts have been devoted towards the electrochemical performance enhancement of MoS_2 anode for LIBs (Wang et al. 2013; Sen and Mitra 2013; Zhao et al. 2014; Zhang et al. 2012). For example, nanostructured MoS_2 materials have been extensively explored. Due to its nanostructure, this system provides a facile strain relaxation during structure/volume change and shortens diffusion paths for Li^+ insertion/deinsertion due to a large contact area with the electrolyte (Zhao et al. 2014; Zhang et al. 2012; Qiu et al. 2010). However, the agglomeration of nanostructured MoS_2 during electrochemical cycling can lead to a rapid loss of the composite conductivity and subsequent capacity decay, which restricts consideration of MoS_2 anode for practical use and commercialization. In our previous works (Zhang et al. 2014a), the advantages of hierarchical architecture towards improving electrochemical response of galvanic cell have been discussed. This promising strategy could be applicable in case of MoS_2 anode, benefiting from the advantages of using single component and providing novel properties due to the synergistic interactions between nanometer-sized building blocks (Hu et al. 2014a). Ding et al. reported that the hierarchical MoS_2 spheres composed of ultrathin nanosheets exhibit a high specific discharged capacity of ~600 mAh g^{-1} at 100 mA g^{-1} after 70 circles (Ding et al. 2012). Li et al. prepared 3D (three-dimensional) flowerlike MoS_2 which exhibits a capacity of ~565 mAh g^{-1} at a current density of 100 mA g^{-1} after 100 circles (Li et al. 2009). However, the hierarchical structured MoS_2 reported in these studies own micrometer dimensions with inhomogeneous distribution of components and particle sizes. These parameters of the system cannot allow for accumulation of the large volume expansion and agglomeration of MoS_2 during charge/discharge cycling, and it shows poor rate performance and low cycling stability.

To overcome this issue, in this study we optimized the size and structure of hierarchical MoS_2, and hierarchically structured MoS_2 microspheres with small (233 nm) and homogeneous particle size were successfully synthesized using a simple hydrothermal process. The nanostructural properties of the obtained MoS_2 microspheres and their electrochemical performance as an anode for a lithium-ion cell were investigated.

Experiment

The synthetic procedures for hierarchical structure of MoS_2 were adopted from the literature (Ma et al. 2013) with some modification. 2.2 g $Na_2MoO_4 \cdot 2H_2O$ (Tianjin Chengyang ≥98 %) and 2.0 g H_2NCSNH_2 (Tianjin Chengyang, ≥99 %) were dissolved in 70 mL deionized water. The aqueous solution was stirred for 10 min, followed by a dropwise addition of 12 M HCl (Tianjin Fuchen, 36–38 %) to adjust the solution pH below 1. The solution was then transferred into a 100 mL Teflon-lined stainless steel autoclave and heated at 200 °C for 24 h. After the autoclave cooled down to room temperature, the resulting MoS_2 precipitate was collected by filtration, and washed using deionized water and ethanol. The resulting black powder was dried for 24 h at 60 °C.

The morphologies and structure of the MoS_2 sample were characterized using scanning electron microscopy (SEM, S-4800, Hitachi Limited), selected area electron diffraction (SAED, JEM-2100F, JEOL), and high-resolution transmission electron microscopy (HRTEM, JEM-2100F, JEOL) at an accelerating voltage of 160 kV. The crystalline phases of the sample were determined by Powder X-ray diffraction (XRD, smart lab, Rigaku Corporation) equipped with Cu Kα radiation. The Brunauer–Emmett–Teller (BET) specific surface area of the sample was detected

at 77 K using Micromeritics Tristar 3000 analyzer. The pore size distribution was calculated based on Barrett–Joyner–Halanda (BJH) model.

The electrochemical performance of the MoS_2 sample was investigated using coin cells (CR2025), with metallic Li as counter and reference electrodes, microporous polypropylene as a separator, and 1 M $LiPF_6$ in a mixture of ethylene carbonate/dimethyl carbonate/ethylenemethyl carbonate with a volume ratio of 1:1:1 as an electrolyte. The working electrode was prepared by mixing MoS_2, carbon black, and polyvinylidene fluoride (PVDF) (Kynar, HSV900) in 1-methyl-2-pyrrolidone (NMP, Sigma-Aldrich, ≥99.5 % purity) in a weight ratio of 8:1:1. The resultant slurry was uniformly spread onto nickel foam using a doctor blade and dried in a vacuum oven at 50 °C for 12 h, and was cut into circular electrodes with 1 cm in diameter. The active material loading in each electrode was 2 mg cm^{-2}. The cells were assembled in an Ar (99.9995 %)-filled glove box (MBraun). Galvanostatic cycling of the cells were carried out on a multichannel battery tester (BTS-5V5 mA, Neware) within a cut-off potential window of 0.001–3.0 V versus Li^+/Li. Cyclic voltammetry (CV) measurements were conducted at 0.5 mV s^{-1} with a potentiostat (VMP3, Biologic) between 0 and 3.0 V versus Li^+/Li. All electrochemical measurements were performed at room temperature.

Results and discussion

Hierarchical MoS_2 microspheres were synthesized by hydrothermal synthesis method. The reaction mechanism can be expressed as follows (Ma et al. 2013):

$$NH_2CSNH_2 + 2H_2O = 2NH_3 \uparrow + H_2S + CO_2 \uparrow$$

$$4Na_2MoO_4 + 9H_2S + 6HCl = 4MoS_2 + Na_2SO_4 + 12H_2O + 6NaCl$$

The schematic of formation of hierarchical MoS_2 microspheres is illustrated in Fig. 1a. The MoS_2 cores are formed via a reaction of Na_2MoO_4 and H_2S. Strong ionic/covalent force leads to the growth of the two-dimensional MoS_2 nanosheets. Ultimately, the growing MoS_2 nanosheets overlap and assemble hierarchical microsphere structure of MoS_2 due to the Van der Waals interactions (Liang et al. 2013). Figure 1b shows the XRD patterns of the MoS_2 product. The diffraction peaks at 11.8°, 32.6°, 43.6°, 57.8° can be indexed as crystalline planes of (002), (100), (103), (110) for hexagonal MoS_2 (JPDS No. 37-1492). All of

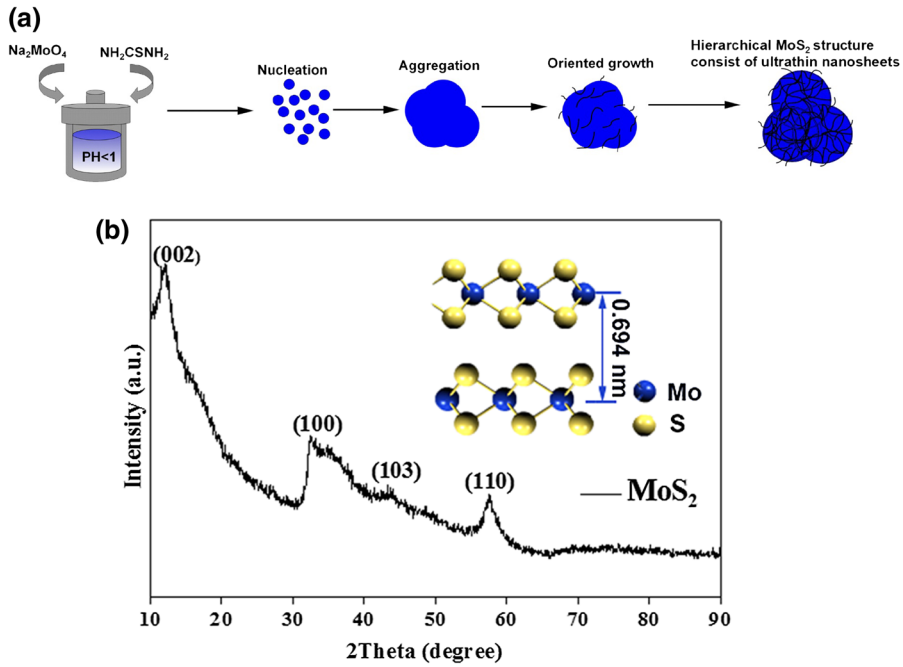

Fig. 1 **a** Schematics of preparation of the hierarchical MoS_2 microspheres; **b** XRD pattern of the hierarchical MoS_2 microspheres; *inset* atomic structure model of MoS_2

the diffraction peaks are weak, indicating a lower crystallinity of the MoS_2 material due to the fact that the material was not annealed; this feature does not affect the electrochemical performance of as-prepared MoS_2 (Qian et al. 2015). The diffraction peak at 11.8°, corresponding to the MoS_2 crystalline plane (002), is lower than that of the hexagonal MoS_2 ($2\theta = 14.4°$, $d = 0.615$ nm). Moreover, the atomic structure model of as-prepared MoS_2 (inset of Fig. 1b) can be described as a sandwich-like structure of S–Mo–S (Haesuk et al. 2011). The average interlayer distance of the prepared MoS_2 nanosheets, calculated according to Bragg's equation, is 0.694 nm. This is larger than that of the crystalline plane 002 (0.615 nm), which was caused by the formation of a new lamellar structure of MoS_2 during the hydrothermal process, demonstrating that the space between the neighboring planes is extended (Xie et al. 2013; Hu et al. 2014b). The enlarged interplanar spacing shortens the path length and provides enhanced channeling for Li-ions diffusion (Liu et al. 2012b).

The porous structure of the hierarchical MoS_2 microspheres was confirmed by nitrogen adsorption/desorption isotherms (Fig. 2a) and pore size distribution analysis (Fig. 2b). It can be seen from these figures the isotherms present a typical type IV adsorption with a hysteresis loop at a relative pressure of 0.45, corresponding to the mesoporous structured material. Furthermore, the pore size distribution (Fig. 2b), calculated based on BJH model, presents a significant ratio of pore size distributed around 3.2 nm, which confirms our suggestion on mesoporous features of the prepared material. This structure of the hierarchical MoS_2 microspheres has resulted in a high BET specific area of 92 $m^2\ g^{-1}$ compared with other MoS_2 materials (Hu et al. 2014b; Xia et al. 2016; Li et al. 2015). It was found that the pore volume for this sample is 0.271 $cm^3\ g^{-1}$ with the average pore size of 6.1 nm, which could also be attributed to the hierarchical structure and highly developed interlaces of the ultrathin nanosheets. These structure and morphology specifics can strongly affect the electrochemical performance of the materials providing rapid electrolyte transport, carrier-ion diffusion, and accommodating the volume changes upon electrochemical cycling.

Figure 3a presents the SEM images of as-prepared MoS_2. It can be seen that the hierarchically structured MoS_2 was successfully synthesized, featuring homogeneous MoS_2 microsphere morphology. These hierarchical MoS_2 microspheres are made up by ultrathin nanosheets with a thickness less than 16 nm as it was shown by the high magnification SEM image (inset of Fig. 3a). Figure 3b presents the particle size distribution for the prepared material. It can be seen that the MoS_2 microspheres present homogeneous particle size distribution with the dominant sizes in a range of 200–260 nm, and average size of 233 nm. These particular structural properties offer enlarged surface area for fast lithium diffusion and enable buffering the volume changes during lithium insertion/deinsertion (Hu et al. 2014b).

The magnified TEM image (Fig. 3c) shows the stacks and clusters of MoS_2 nanosheets. The SAED patterns (inset of Fig. 3c) exhibit three distinct diffraction rings which can be indexed as the different lattice planes of the hexagonal MoS_2. The lattices of MoS_2 microspheres can be identified by the HRTEM image presented in Fig. 3d. The lattice d-spacing is calculated to be 0.694 nm, and can be indexed as the

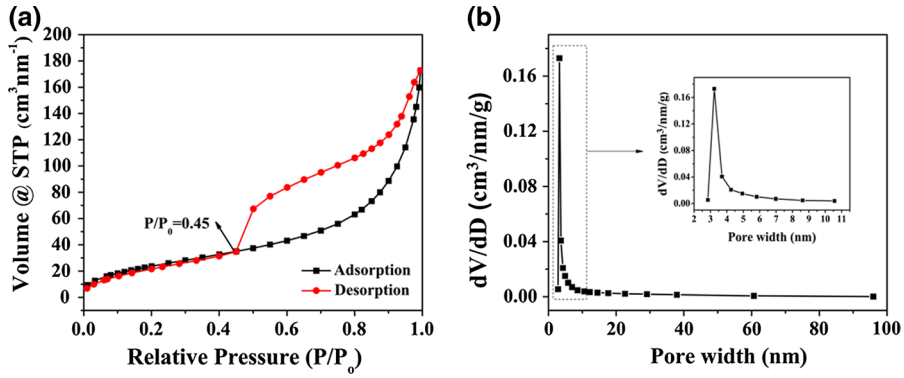

Fig. 2 **a** Nitrogen adsorption/desorption isotherms; **b** pore size distribution of the hierarchical MoS_2 microspheres. *Inset* magnification of pore size distribution between 2 and 10.0 nm

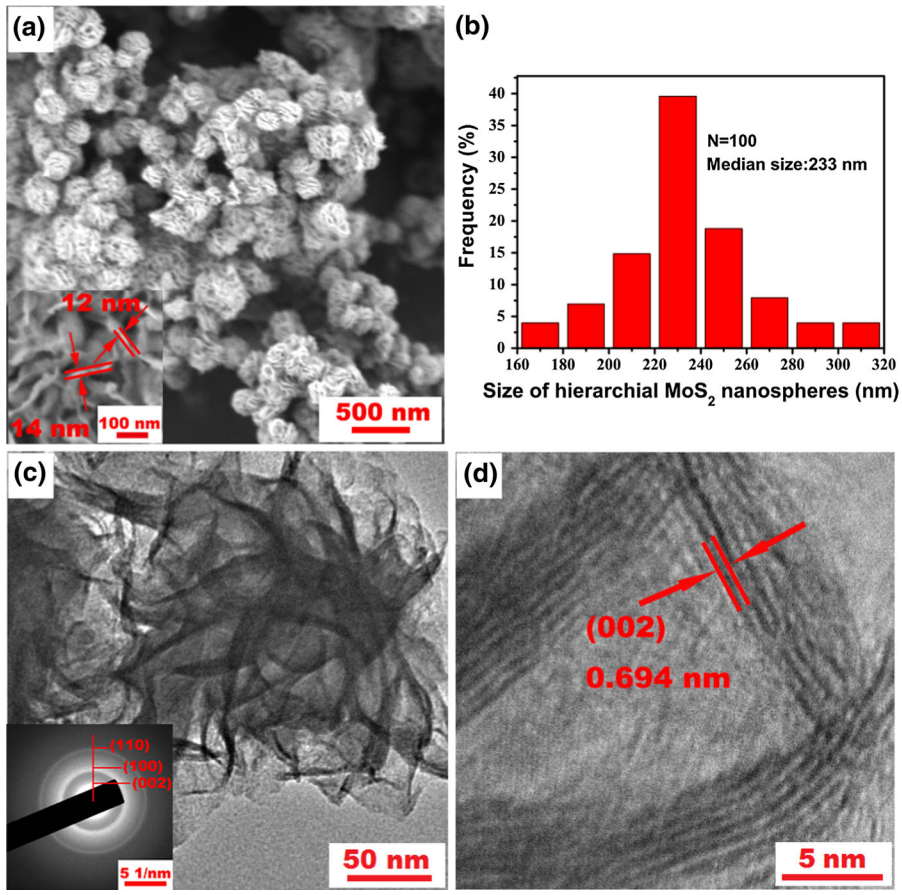

Fig. 3 **a** Low magnification SEM of the hierarchical MoS_2 microspheres; *inset* high magnification SEM of the hierarchical MoS_2 microspheres; **b** particle size distribution of the hierarchical MoS_2 microspheres; **c** TEM of the hierarchical MoS_2 microspheres, *inset* SAED pattern of the hierarchical MoS_2 microspheres; **d** HRTEM of the hierarchical MoS_2 microspheres

(002) plane of MoS_2. The interplanar spacing of 0.694 nm is enlarged compared with the hexagonal MoS_2 (0.615 nm), and corresponds with the XDR result.

The electrochemical performance of the hierarchical MoS_2 microspheres as anode material for LIBs was investigated in lithium half cells. Figure 4 shows the initial cyclic voltammogram (CV) of the hierarchical MoS_2 microspheres at a scan rate of 0.5 mV s^{-1}. During the initial discharge cycle, two oxidation peaks were observed at $\sim$0.33 and $\sim$0.95 V *vs.* Li^+/Li, respectively. A peak at $\sim$0.95 V could be related to a process of formation of Li_xMoS_2 upon Li-ions intercalation into MoS_2, whereas a peak at $\sim$0.33 V could be associated with the MoS_2 conversion process via $Li_xMoS_2 \rightarrow Li_2S + Mo/Li_y$ and formation of solid electrolyte interphase (SEI) due to the electrolyte decomposition (Sen and Mitra 2013; Hu et al. 2014b; Liu et al. 2012b). During the first anodic sweep, a low intensity peak at $\sim$1.64 V could be a reflection of the Mo $\rightarrow$ MoS_2 conversion process, and an obvious peak at $\sim$2.35 V corresponds to the oxidation process of sulfur $Li_2S \rightarrow S$ (Xiao et al. 2011). In the following

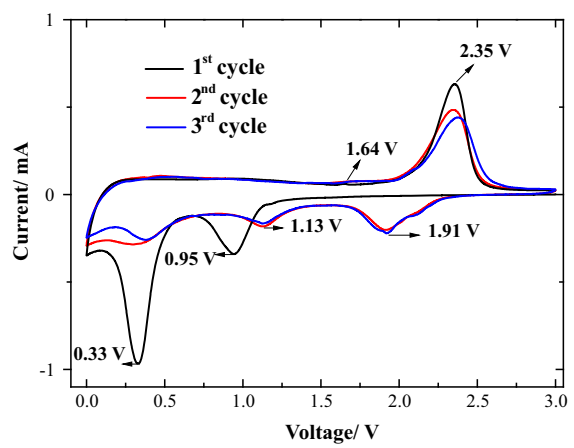

Fig. 4 CV profiles of the hierarchical MoS_2 microsphere anode

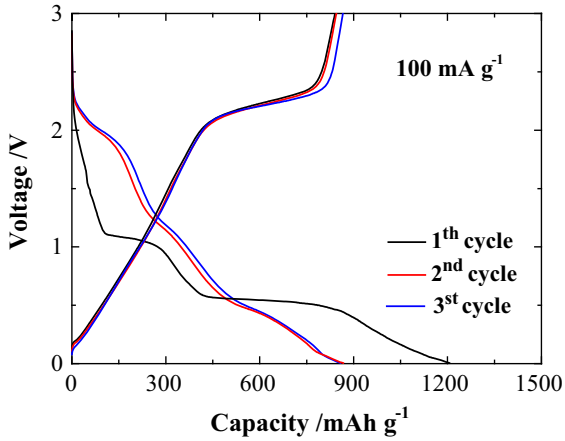

Fig. 5 Charge–discharge profiles of the hierarchical MoS_2 microsphere anode at 100 mA g^{-1}

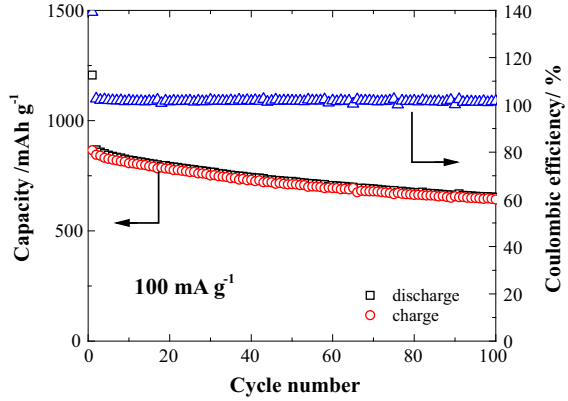

Fig. 6 Cyclability of the hierarchical MoS_2 microsphere anode at 100 mA g^{-1}

cycles, a peak at ~0.33 V diminishes, indicating irreversible character of the SEI formation. New peaks appear at ~1.91 and ~1.13 V, which might result from conversion of S to LiS_2 and association of Li with Mo, respectively. Figure 5 shows the charge–discharge curves of the hierarchical MoS_2 microspheres at a current density of 100 mA g^{-1}, and consists of two potential plateaus at ~0.55 and ~1.08 V, indicating the two-step lithiation reaction of MoS_2. It should be noted that the initial discharge curve has a prolonged feature which could be due to the formation of SEI and related irreversible energy loss. In the following discharge curves, the plateaus observed in the first discharge shift towards the higher potentials of ~1.15 and ~1.94 V, respectively, which could be due to the completion of the SEI formation and electrochemical activation of the system (Wang et al. 2013). The hierarchical MoS_2 microsphere system shows a highly reversible electrochemical property, which is indicated by nearly overlapping potential profiles starting from the 2nd cycle (see Fig. 5). The results of charge–discharge curves of the hierarchical MoS_2 microspheres correspond well with the CV results discussed above.

Figure 6 presents both the cyclic performance and the coulombic efficiency data for the hierarchical MoS_2 microsphere electrode. It can be seen that this material exhibits a stable cycling ability at a current density of 100 mA g^{-1}, and after 100 cycles it retains a capacity of 653 mAh g^{-1}, which is about 75 % of the second discharge capacity. Along with this excellent cycling performance, the hierarchical MoS_2 microsphere electrode exhibits a high coulombic efficiency of about 100 %. This performance enhancement of the material could be attributed to large specific area and increased interplanar spacing of the (002) crystal plane of the MoS_2 microspheres, which increases the area of the interface between electrode and electrolyte, and thus provides more active sites for the Li-ion insertion/desertion (Zhang et al. 2014b; Qian et al. 2015). Secondly, the hierarchical nanosheet structure of MoS_2 buffers the volume expansion and destruction of the electrode during the lithiation–delithiation processes (Zhang et al. 2014c).

The ability of an electrode material to operate within a wide range of current densities or charge–discharge rates is another important property-determining perspectives of its practical application. Therefore, the rate capability of the hierarchical MoS_2 microspheres was studied at different current densities. Figure 7 presents the rate capability data. It can be seen that the hierarchical MoS_2 microspheres possess a high capacity of 836 mAh g^{-1} at a current density of 100 mA g^{-1} after the first ten cycles. With an increase in current density to 200 and 500 mA g^{-1}, the discharge capacity of the electrode gradually decreases to 770 and 681 mAh g^{-1}, respectively. The cell could still maintain a high capacity of 480 mAh g^{-1} even at a high current density of 1000 mA g^{-1}. Upon reducing the current density back to 100 mA g^{-1}, the cell regains its capacity and exhibits a stable cycling at a value of 814 mAh g^{-1} up to 60 cycles. The improved rate and cycling performance of the material can be resulted from the shortened lithium-ion diffusion distance and an enhanced

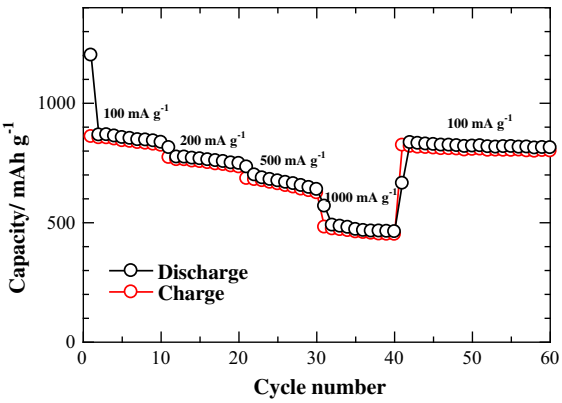

Fig. 7 Rate capability of the hierarchical MoS_2 microsphere anode

structural stability of the hierarchical MoS_2 microspheres. Furthermore, the electrochemical performance of our hierarchical MoS_2 microsphere electrode was compared with that of the MoS_2-based anodes reported in the literature (Table 1). It can be seen that a remarkably enhanced performance was achieved for the hierarchical MoS_2 anode in the present study.

The results of the studies on the hierarchical MoS_2 microspheres in the present work provide insights into the design of desirable structures of the material and preparing its hybrids and composites with other materials, such as carbon nanotubes, graphene, and other carbonaceous framework systems. Graphene-based MoS_2 composite exhibits enhanced reversible capacity and smaller capacity degradation due to graphene's desirable chemical stability and high conductivity (Chang et al. 2013; Xiang et al. 2016). Therefore, the present work could be considered as a step towards in an advanced research on a new approach to prepare hierarchically structured MoS_2-based composites with excellent electrochemical performance for lithium-ion batteries.

Conclusions

In this work, nanosized (~233 nm) and homogeneously distributed hierarchical MoS_2 microspheres were fabricated via a simple cost-effective hydrothermal synthesis method. The crystalline phases and morphology of the material were characterized by XRD, SEM, TEM, and HRTEM methods. It was shown that the prepared hierarchical MoS_2 microspheres are composed of ultrathin nanosheets with an extended interlayer spacing. Hierarchical MoS_2 microspheres with such unique structural characteristics possess enlarged specific surface area and are able to accommodate the significant volume changes upon lithium insertion/deinsertion. Electrochemical performance tests showed that the hierarchical MoS_2 microspheres could deliver a high specific capacity of 653 mAh g^{-1} at 100 mA g^{-1} after 100 cycles. Furthermore, it can reach a very high capacity of 480 mAh g^{-1} even at an elevated current density of 1000 mA g^{-1}. These excellent lithium storage properties of the hierarchical MoS_2 microspheres are believed to be contributed by its small and homogeneous size as well as the enlarged layer distance of

Table 1 Comparison of the electrochemical data for MoS_2-based anode for Li-ion batteries in present work and published in the literature

Material	Reversible capacity (mAh g^{-1})	Cycle number	Current density (mA g^{-1})	Refs.
MoS_2–RGO composites	305	50th	100	Fei et al. (2013)
Hierarchical MoS_2 microspheres	~600	70th	100	Ding et al. (2012)
Flowerlike MoS_2	~565	100th	100	Li et al. (2009)
MoS_2 nanosheets on Carbon nanotubes	539.9–504.6	100th	50	Haesuk et al. (2011)
MoS_2 nanotubes	770	40th	40	Feng et al. (2009)
Mesoporous MoS_2	630	20th	35	Fang et al. (2009)
Hierarchical MoS_2 microspheres	745	50th	100	Our work
	653	100th	100	

(002) crystal plane, and make this material a promising candidate anode for lithium-ion batteries.

Acknowledgments The authors acknowledge the financial support from the National Natural Science Foundation of China (Grant No. 21406052), the Program for the Outstanding Young Talents of Hebei Province (Grant No. BJ2014010), Natural Science Foundation of Hebei Province of China (Project No. E2015202037), and Science and Technology Correspondent Project of Tianjin (Project No. 14JCTPJC00496). ZB acknowledges the research grant 4649/GF from the Ministry of Education and Science of Kazakhstan.

References

Birrozzi A, Raccichini R, Nobili F, Marinaro M, Tossici R, Marassi R (2014) High-stability graphene nano sheets/SnO_2 composite anode for lithium ion batteries. Electrochim Acta 137:228–234

Chang K, Geng D, Li X, Yang J, Tang Y, Cai M, Li R, Sun X (2013) Ultrathin MoS_2/Nitrogen-Doped Graphene Nanosheets with Highly Reversible Lithium Storage. Adv Energy Mater 3:839–844

Ding S, Zhang D, Chen JS, Lou XW (2012) Facile synthesis of hierarchical MoS_2 microspheres composed of few-layered nanosheets and their lithium storage properties. Nanoscale 4:95–98

Fang X, Yu X, Liao S, Shi Y, Hua YS, Wang Z, Stucky GD, Chen L (2012) Lithium storage performance in ordered mesoporous MoS_2 electrode material. Micropor Mesoporous Mat 151:418–423

Fei L, Lin QL, Yuan B, Chen G, Xie P, Li YL, Xu Y, Deng SG, Smirnov S, Luo HM (2013) Reduced graphene oxide wrapped fes nanocomposite for lithium-ion battery anode with improved performance. ACS Appl Mater Inter 5:5330–5335

Feng C, Jun Ma, Li H, Zeng R, Guo Z, Liu H (2009) Synthesis of molybdenum disulfide (MoS_2) for lithium ion battery applications. Mater Res Bull 44:1811–1815

Gu Y, Xu Y, Wang Y (2013) Graphene-wrapped CoS nanoparticles for high-capacity lithium-ion storage. ACS Mater Inter 5:801–806

Haesuk H, Hyejung K, Jaephil C (2011) MoS_2 nanoplates consisting of disordered graphene-like layers for high rate lithium battery anode materials. Nano Lett 11:4826–4830

Hu G, Cao J, Peng Z, Cao Y, Du K (2014a) Enhanced high-voltage properties of $LiCoO_2$ coated with $Li[Li_{0.2}Mn_{0.6}Ni_{0.2}]O_2$. Electrochim Acta 149:49–55

Hu L, Ren Y, Yang H, Xu Q (2014b) Fabrication of 3D hierarchical $MoS_{(2)}$/polyaniline and $MoS_{(2)}$/C architectures for lithium-ion battery applications. ACS Appl Mater Inter 6:14644–14652

Lai C, Lu M, Chen L (2012) Metal sulfide nanostructures: synthesis, properties and applications in energy conversion and storage. J Mater Chem 22:19–30

Li H, Li W, Ma L, Chen W, Wang J (2009) Electrochemical lithiation/delithiation performances of 3D flowerlike MoS_2. J Alloy Compd 471:442–447

Li J, Hou Y, Gao X, Guan D, Xie Y, Chen J, Yuan C (2015) A three-dimensionally interconnected carbon nanotube/layered MoS2 nanohybrid network for lithium ion battery anode with superior rate capacity and long-cycle-life. Nano Energy 16:10–18

Liang S, Zhou J, Liu J, Pan A, Tang Y, Chen T, Fang G (2013) PVP-assisted synthesis of MoS_2 nanosheets with improved lithium storage properties. Cryst Eng Comm 15:4998–5002

Liu H, Su D, Wang G, Qiao S (2012a) An ordered mesoporous WS_2 anode material with superior electrochemical performance for lithium ion batteries. J Mater Chem 22:17437–17440

Liu H, Su DW, Zhou RF, Sun B, Wang GX, Qiao SZ (2012b) Highly Ordered Mesoporous MoS_2 with Expanded Spacing of the (002) Crystal Plane for Ultrafast Lithium Ion Storage. Adv Energy Mater 2:970–975

Ma G, Peng H, Mu J, Huang H, Zhou X, Lei Z (2013) In situ intercalative polymerization of pyrrole in graphene analogue of MoS_2 as advanced electrode material in supercapacitor. J Power Sources 229:72–78

Qian X, Wang Y, Zhou W, Zhang L, Song G (2015) Interlayer distance dependency of lithium storage in MoS_2 as anode material for lithium-ion batteries. Int J Electrochem Sci 10:3510–3517

Qiu M, Yang L, Qi X, Li J, Zhong J (2010) Fabrication of ordered NiO coated Si nanowire array films as electrodes for a high performance lithium ion battery. ACS Appl Mater Inter 2:3614–3618

Sen UK, Mitra S (2013) High-rate and high-energy-density lithium-ion battery anode containing 2D MoS_2 nanowall and cellulose binder. ACS Appl Mater Inter 5:1240–1247

Vaughn DD, Hentz OD, Chen S, Wang D, Schaak RE (2012) Formation of SnS nanoflowers for lithium ion batteries. Chem Commun 48:5608–5610

Wang M, Li G, Xu H, Qian Y, Yang J (2013) Enhanced lithium storage performances of hierarchical hollow MoS_2 nanoparticles assembled from nanosheets. ACS Appl Mater Inter 5:1003–1008

Xia Y, Wang B, Zhao X, Wang G, Hui Wang (2016) Core-shell composite of hierarchical MoS2 nanosheets supported on graphitized hollow carbon microspheres for high performance lithium-ion batteries. Electrochim Acta 187:55–64

Xiang J, Dong D, Wen F, Zhao J, Zhang X, Wang L, Liu Z (2016) Microwave synthesized self-standing electrode of MoS_2 nanosheets assembled on graphene foam for high-performance Li-Ion and Na-Ion batteries. J Alloy Compd 660:11–16

Xiao J, Wang X, Yang XQ, Xun S, Liu G, Koech PK, Liu J, Lemmon JP (2011) Electrochemically induced high capacity displacement reaction of PEO/MoS_2/graphene nanocomposites with lithium. Adv Funct Mater 21:2840–2846

Xie J, Zhang J, Li S, Grote F, Zhang X, Zhang H, Wang R, Lei Y, Pan B, Xie Y (2013) Controllable disorder engineering in oxygen-incorporated MoS_2 ultrathin nanosheets for Efficient hydrogen evolution. J Am Chem Soc 135:17881–17888

Zhang Y, Zhao Y, Sun K, Chen P (2011) Development in lithium/sulfur secondary batteries. Open Mater Sci J 5:215–221

Zhang C, Wang Z, Guo Z, Lou XW (2012) Synthesis of MoS_2-C one-dimensional nanostructures with improved lithium storage properties. ACS Appl Mater Inter 4:3765–3768

Zhang Y, Zhao Y, Bakenov Z, Tuiyebayeva M, Konarov A, Chen P (2014a) Synthesis of hierarchical porous sulfur/polypyrrole/multiwalled carbon nanotube composite cathode for lithium batteries. Electrochim Acta 143:49–55

Zhang S, Yu XB, Yu HL, Chen YJ, Gao P, Li CY, Zhu CL (2014b) Growth of ultrathin $MoS_{(2)}$ nanosheets with expanded spacing of (002) plane on carbon nanotubes for high-performance sodium-ion battery anodes. ACS Appl Mater Inter 6:21880–21885

Zhang L, Wu HB, Yan Y, Wang X, Lou X (2014c) Hierarchical MoS_2 microboxes constructed by nanosheets with enhanced electrochemical properties for lithium storage and water splitting. Energy Environ Sci 7:3302–3306

Zhao Y, Zhang Y, Gosselink D, Sadhu M, Cheang H-J, Chen P (2012) Polymer electrolytes for lithium/sulfur batteries. Membranes 2:553–564

Zhao CY, Kong JH, Yao XY, Tang XS, Dong YL, Phua SL, Lu XH (2014) Thin MoS_2 nanoflakes encapsulated in carbon nanofibers as high-performance anodes for lithium-ion batteries. ACS Appl Mater Inter 6:6392–6398

Zhong H, Yang G, Song H, Liao Q, Cui H, Shen P, Wang CX (2012) Vertically aligned graphene-like SnS_2 ultrathin nanosheet arrays: excellent energy storage, catalysis, photoconduction, and field-emitting performances. J Phys Chem C 116:9319–9326